

Supplemental Material for
Ferroelectricity in Charge-Ordering Crystals with Centrosymmetric Lattices

Yali Yang(杨亚利)^{1,2}, Laurent Bellaiche³ and Hongjun Xiang(向红军)^{1,2*}

¹Key Laboratory of Computational Physical Sciences (Ministry of Education), State Key Laboratory of Surface Physics, and Department of Physics, Fudan University, Shanghai 200433, People's Republic of China

²Shanghai Qizhi Institution, Shanghai 200232, People's Republic of China

³Physics Department and Institute for Nanoscience and Engineering, University of Arkansas, Fayetteville, Arkansas 72701, USA

CONTENTS

I. Computational methods	2
II. Three-dimensional breathing mode in BaBiO₃	2
III. Ferroelectric switching in BaBiO₃ under different electric fields	3
IV. Zero contribution from the breathing mode to ferroelectricity in BaBiO₃	4
V. Wannier functions of Bi 6s electrons during ferroelectric switching	5

* hxiang@fudan.edu.cn

I. Computational methods

All density functional theory (DFT) calculations are performed with the Vienna *ab-initio* Simulation Package (VASP).^[1] The generalized gradient approximation (GGA)^[2] in the form of the revised Perdew-Burke-Ernzerhof functional (PBEsol)^[3] and the projector augmented wave (PAW) method^[4] are applied to describe the exchange-correlation and the core electrons, respectively. The plane-wave cutoff and convergence criteria for energy and force are set to be 550 eV, 10^{-7} eV, and 0.001 eV/Å, respectively. The Ba: $5s^25p^66s^2$, Bi: $5d^{10}6s^26p^3$ and O: $2s^22p^4$ are treated as valence electrons. A $6 \times 6 \times 4$ Monkhorst-Pack k-mesh is adopted for integrations within the Brillouin zone. The transition path from one ferroelectric (FE) state to another FE state is obtained using the climbing image nudged elastic band method (cNEB) as implemented in the VASP package.^[5, 6] The maximally localized Wannier functions (MLWFs) are obtained using the wannier90 program.^[7]

II. Three-dimensional breathing mode in BaBiO₃

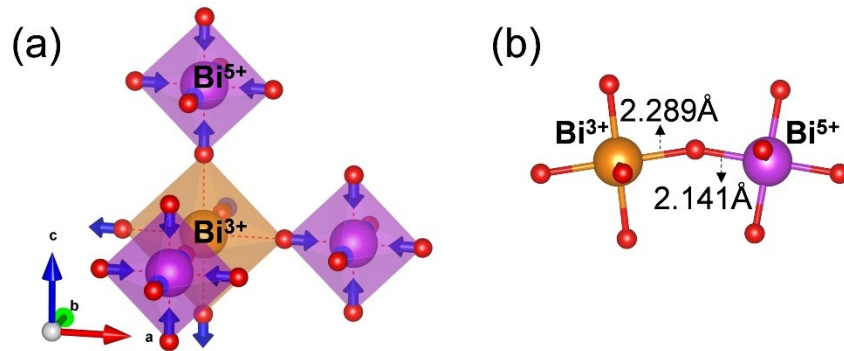


Figure S1. (a) Sketch of the three-dimensional breathing mode in BaBiO₃ system, with blue arrows indicating the distortion of O atoms. Only four corner-shared octahedra are selected to present. (b) Bond lengths of Bi³⁺-O²⁻ and Bi⁵⁺-O²⁻ bonds along the [-110] direction of the optimized $P2_1/n$ structure in Figure 2(c) of the main text.

III. Ferroelectric switching in BaBiO₃ under different electric fields

As mentioned in the main text that the change in polarization between the two FE states in the BaBiO₃ system is closely related to the transition path: different paths between the two FE states lead to different changes in polarization, not only the polarization direction but also the magnitude (see Fig. S2). Such phenomenon can hardly happen in conventional FEs, because there (e.g., BaTiO₃) the transition path with the smallest polarization change generally has the lowest energy barrier. It is difficult for heavy cations (e.g., Ti⁴⁺) to move freely under the external electric field.

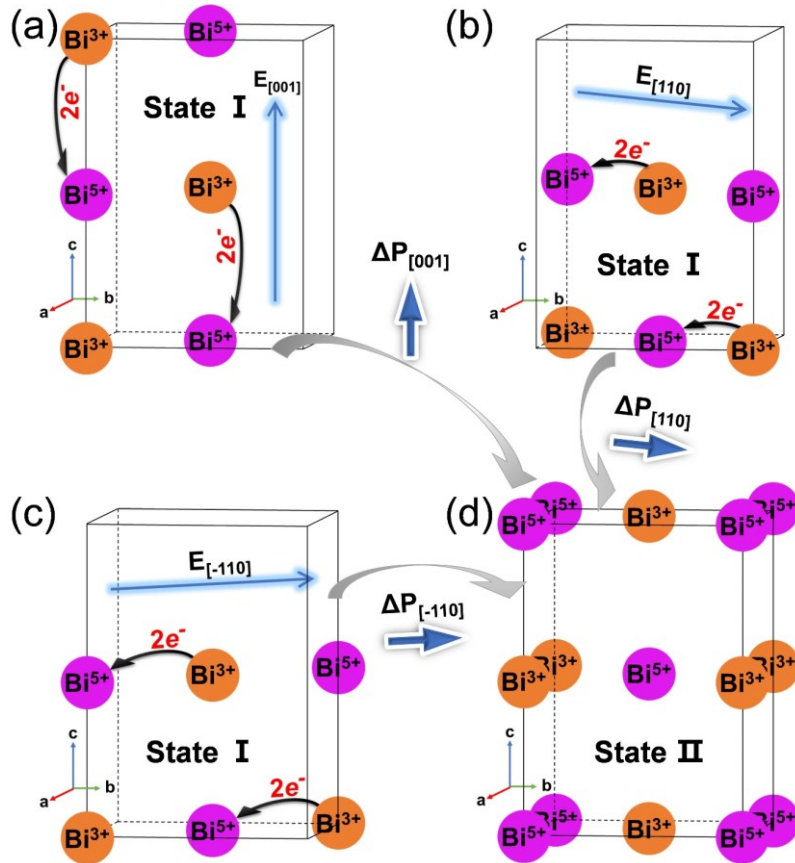


Figure S2. Schematic of ferroelectric switching from (a)-(c) state I to (d) state II of three-dimensional charge-ordering BaBiO₃ system under different external electric fields. Note that only Bi³⁺ (orange ball) and Bi⁵⁺ (purple ball) cations are shown for clarity. The straight light and dark blue arrows indicate the direction of the electric field and polarization, respectively. The black curved arrows indicate the electronic transfer under the electric fields. The grey curved arrows indicate the transition from state I to state II.

IV. Zero contribution from the breathing mode to ferroelectric polarization in BaBiO₃

As mentioned in the main text, the motions of the oxygen atoms in the BaBiO₃ system during the FE switching do not induce polarization. To address this point more clearly, let us consider a simple model (see Fig. S3). We would like to calculate the change in polarization between FE state I and state II (see Fig. S3). One can view the transition between state I and state II as a two-step process. The first step (i.e., from state I to state I') is the electronic transfer and the second (i.e., from state I' to state II) is the ionic motions due to the breathing mode. Thus, state I' can be considered as an “intermediate” state between state I and state II. The unit cell is adopted to also contain two A atoms and two B atoms as that in Fig. 1 of the main text. Now the B atoms in the two FE states are not at the middle of the two adjacent A atoms but are at a distance of l from the nearest Aⁿ⁺ cations. Then, the change of polarization (in fact the dipole moment in unit of $e \cdot \text{\AA}$) from state I to state II is

$$\Delta P = P_{II} - P_I$$

where $(P_{I'} - P_I) = -\frac{(n-m)a}{2}$ is the change of polarization solely due to the electronic transfer as we discussed in the main text, while $(P_{II} - P_{I'})$ is the change of polarization due to the displacements of the B anions. One can easily see that $P_{II} - P_{I'} = 0$ as the left B anion and the right B anion displace along the opposite directions for a given A cation. Finally, the change of polarization from state I to state II is

$$\Delta P = P_{II} - P_I = -\frac{(n-m)a}{2}.$$

This analysis clearly shows that the change in polarization in the centrosymmetric charge-ordering system originates solely from the electronic transfer between the two FE states, suggesting that the breathing mode distortions do not contribute to the polarization. This result can be understood in another way: the breathing mode in centrosymmetric charge-ordering systems (e.g., BaBiO₃) is not a FE distortion mode at the Γ point of the Brillouin zone.

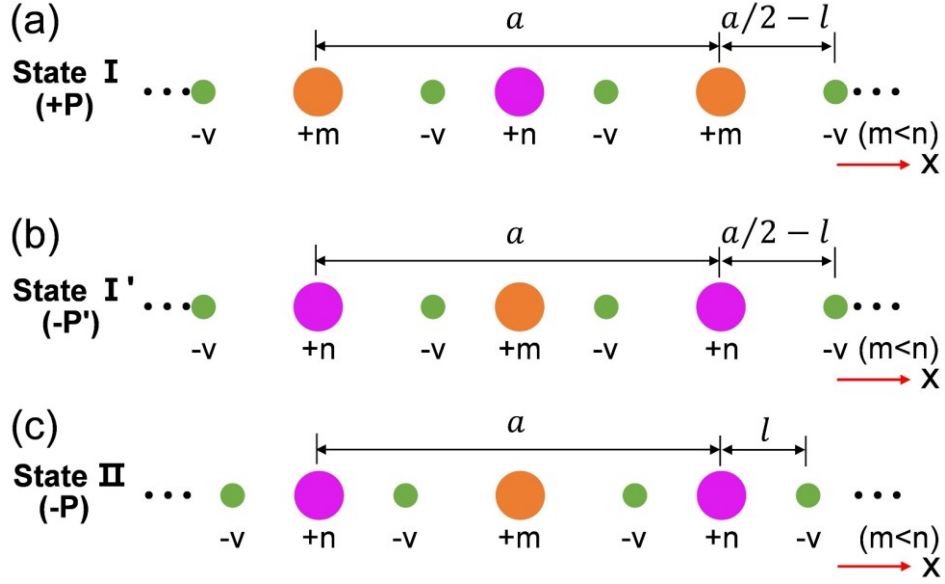


Figure S3. Schematic of the two symmetrically equivalent FE states (a) state I and (c) state II of the one-dimensional binary charge-ordering system AB. State I' in (b) is an “intermediate” state between state I and state II. The A^{m+} , A^{n+} , and B^{v-} ions are indicated by orange, purple, and green balls, respectively. a is the lattice constant of the unit cell which includes two A and two B atoms, and l is the distance between B^{v-} and their nearest A^{n+} ions in the two FE states.

V. Wannier functions of Bi 6s electrons during ferroelectric switching

To investigate the electronic properties of BaBiO_3 , e.g., the electronic transfer during the ferroelectricity switching, we calculate the maximally localized Wannier functions for the two FE states. As shown in Fig. S4(a), the band structure for FE state I is calculated. The calculated band gap is almost zero due to the fact that the PBEsol functional normally underestimates the band gaps. Therefore, the Heyd-Scuseria-Ernzerhof (HSE06) hybrid functional is then used to calculate the band gap of BaBiO_3 based on the PBEsol optimized structure. We find that the HSE06 functional can correctly reveal the insulation property of BaBiO_3 , and the calculated band gap is about 0.47 eV, in agreement with the experimentally observed insulating nature of BaBiO_3 . We consider all occupied Wannier functions to find that the valence band structures from the DFT calculations are reproduced quite well. Since we know that the Bi $6s^2$ electrons transfer from Bi^{3+} to Bi^{5+} cations during the ferroelectricity switching, we calculate the Wannier functions of all the occupied 6s orbitals of Bi^{3+} in state I and state II. The results are shown in Figs. S4(b)-(e). It is clear that the 6s electrons in the FE states are mainly distributed around the Bi^{3+} cations [see the

orange balls in Fig. S4(b)-(e)]. Such results clearly show the transfer of the $6s^2$ electrons from Bi^{3+} to Bi^{5+} cations, leading to the ferroelectricity switching from FE state I to FE state II via the transition state.

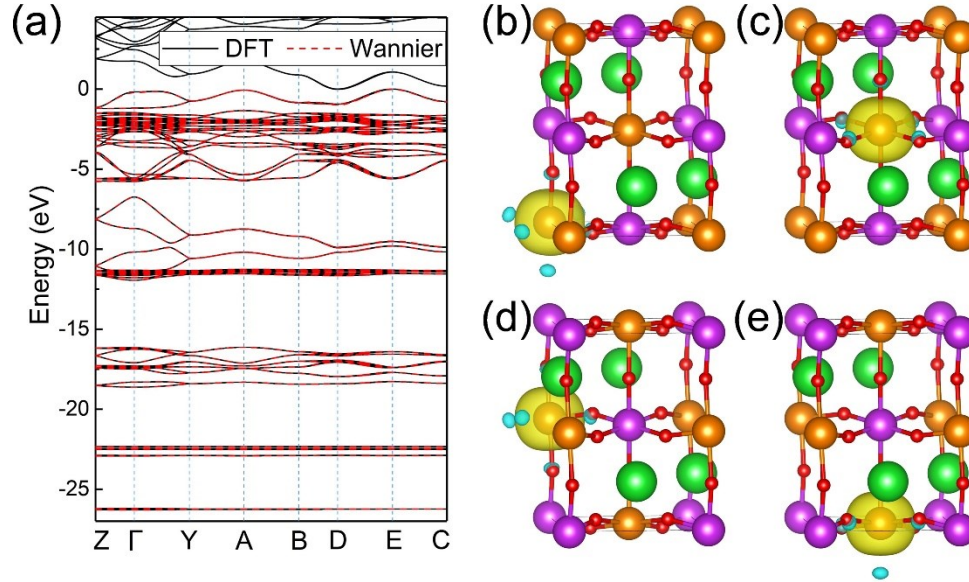


Figure S4. (a) Band structure of FE state I (in $P2_1/n$ symmetry) of BaBiO_3 . (b)-(c) Wannier functions of the Bi^{3+} $6s^2$ electrons in state I. (d)-(e) Wannier functions of the Bi^{3+} $6s^2$ electrons in state II. Note that, different from the DFT band calculation, only the occupied bands are calculated via Wannier calculations.

References

- [1] Kresse G and Joubert D 1999 *Phys. Rev. B* **59** 1758
- [2] Perdew J P, Burke K and Ernzerhof M 1996 *Phys. Rev. Lett.* **77** 3865
- [3] Perdew J P, Ruzsinszky A, Csonka G I, Vydrov O A, Scuseria G E, Constantin L A, Zhou X and Burke K 2008 *Phys. Rev. Lett.* **100** 136406
- [4] Blochl P E 1994 *Phys. Rev. B Condens. Matter* **50** 17953
- [5] Henkelman G and Jónsson H 2000 *J. Chem. Phys.* **113** 9978
- [6] Henkelman G, Uberuaga B P and Jónsson H 2000 *J. Chem. Phys.* **113** 9901
- [7] Pizzi G, Vitale V, Arita R, Blugel S, Freimuth F, Geranton G, Gibertini M, Gresch D, Johnson C, Koretsune T, Ibanez-Azpiroz J, Lee H, Lihm J M, Marchand D, Marrazzo A, Mokrousov Y, Mustafa J I, Nohara Y, Nomura Y, Paulatto L, Ponce S, Ponweiser T, Qiao J, Thole F, Tsirkin S S, Wierzbowska M, Marzari N, Vanderbilt D, Souza I, Mostofi A A and Yates J R 2020 *J. Phys. Condens. Matter.* **32** 165902